Quasiprobability using Dual Unitary Circuits

Rohit Kumar Shukla[1, *]

[1] *Department of Chemistry; Institute of Nanotechnology and Advanced Materials; Center for Quantum Entanglement Science and Technology, Bar-Ilan University, Ramat-Gan 5290002, Israel*

(Dated: November 26, 2025)

I. INTRODUCTION

II. SET UP

We consider the ground state of the one-dimensional Ising model with nearest-neighbour interactions in the x direction:

$$H_0 = -J \sum_i \sigma_i^x \sigma_{i+1}^x, \tag{1}$$

whose ground state $|\psi_0\rangle$ is taken as the initial state. At time $t = 0$, we suddenly switch on a transverse magnetic field in the z-direction:

$$H = -J \sum_i \sigma_i^x \sigma_{i+1}^x - h_z \sum_i \sigma_i^z. \tag{2}$$

We compute the Kirkwood–Dirac quasiprobability (KDQP):

$$K_{ab}^{11}(t) = \mathrm{Tr}\left[\Pi_a^1(t)\Pi_b^1(0), \rho_0\right], \tag{3}$$

where Π_a^1 and Π_b^1 are projectors such as $|0\rangle\langle 0|$ and $|1\rangle\langle 1|$.

A. Observed Behaviour of the First Negativity Time

We define t_{neg} as the time at which the KD quasiprobability becomes negative for the first time. The numerical observations are:

1. For $h_z/J < 0.6$: negativity arises from projectors

$$\Pi_a^1 = |1\rangle\langle 1|, \quad \Pi_b^1 = |1\rangle\langle 1|. \tag{4}$$

2. For $h_z/J > 0.6$: negativity arises from

$$\Pi_a^1 = |1\rangle\langle 1|, \quad \Pi_b^1 = |0\rangle\langle 0|. \tag{5}$$

3. At $h_z/J = 0.6$, the value of t_{neg} exhibits a sharp jump.
4. Near $h_z/J = 1$, negativity appears at very small times.

* rohitkrshukla.rs.phy17@itbhu.ac.in

B. Physical Interpretation

The transition between the projectors responsible for negativity reveals how the low-energy excitation structure reorganizes following the quench.

1. *Competition Between x-Order and z-Field*

The initial ground state exhibits strong correlations in the x basis. After the quench, the dynamics reflects competition between:

- the interaction term J—favouring x-alignment,
- the transverse field h_z—favouring z-alignment.

For small h_z, the system remains close to the x-ordered phase, and negativity originates from the $(1, 1)$ sector. For larger h_z, the dynamics is rotated strongly into the z basis, and negativity emerges from the mixed $(1, 0)$ sector.

Thus the boundary near $h_z/J \approx 0.6$ corresponds to a dynamical crossover from interaction-dominated to field-dominated behaviour.

2. *Origin of the Jump at $h_z/J = 0.6$*

Negativity requires:

- generation of coherent superpositions,
- sufficient strength of interference terms.

At the crossover point, the interference pattern is least efficient, causing a large t_{neg}. This resembles critical slowing down, although it is a dynamical crossover rather than a ground-state critical point.

3. *Why t_{neg} Becomes Small Near $h_z/J = 1$*

At this value, the quench is strong and generates rapid phase accumulation between the $|0\rangle$ and $|1\rangle$ components, creating strong interference at early times. This behaviour is reminiscent of resonant dynamical points where eigenfrequencies align with the quench strength.

III. FURTHER PHYSICAL INSIGHTS

A. Dynamical Phase Diagram

The switching of the dominant negativity sector at $h_z/J \approx 0.6$ defines a dynamical crossover line, dividing the evolution into:

- interaction-dominated region (same-projector negativity),
- field-dominated region (mixed-projector negativity).

B. Connection to Lieb–Robinson Bounds

Negativity signals the spread of nonclassical correlations. The change in which projectors generate negativity suggests a reorganization of the effective light-cone velocities in different dynamical regimes.

C. Relation to Dynamical Quantum Phase Transitions (DQPTs)

The sudden rise of negativity near $h_z/J = 1$ may correlate with nonanalyticities in the Loschmidt rate function or Fisher zeros touching the real-time axis. This connection can be further explored.

D. Operational Implications

KD negativity quantifies measurement incompatibility. The switch from $(1,1)$ to $(1,0)$ sectors indicates that the optimal measurement basis for witnessing nonclassicality depends strongly on the quench strength. This may have applications in sensing or in engineering interference-enhanced protocols.

3. Entanglement Measures

We can compute the bipartite entanglement entropy $S_A(t)$ of a subsystem A:

$$S_A(t) = -\mathrm{Tr}\big[\rho_A(t) \log \rho_A(t)\big], \tag{6}$$

where the reduced density matrix of subsystem A is obtained by tracing out the complement $\bar{A}$:

$$\rho_A(t) = \mathrm{Tr}_{\bar{A}}\big[\, |\psi(t)\rangle \langle\psi(t)| \,\big]. \tag{7}$$

Observation: Sharp changes in the entanglement growth often correlate with the *first-negativity time* t_{neg}.

Interpretation: When the projector responsible for KD quasiprobability negativity switches (e.g., from $(1,1)$ to $(1,0)$), it typically corresponds to a change in the dominant entanglement structure in the system.

4. Loschmidt Echo / Dynamical Free Energy

The Loschmidt amplitude is defined as:

$$L(t) = \big|\langle\psi_0|\psi(t)\rangle\big|^2, \tag{8}$$

and the corresponding rate function (dynamical free energy) is

$$g(t) = -\frac{1}{N} \log L(t). \tag{9}$$

Observation: The first-negativity time t_{neg} sometimes aligns with sharp features or inflection points in $g(t)$, indicating that the interference responsible for negativity is linked to low-energy excitation rearrangements.

5. Occupation in the Instantaneous Eigenbasis

After diagonalizing the Hamiltonian H (post-quench):

$$H = \sum_n E_n \, |n\rangle \langle n| \,, \tag{10}$$

one can compute the occupation probabilities in the instantaneous eigenbasis:

$$p_n(t) = \big|\langle n|\psi(t)\rangle\big|^2. \tag{11}$$

Observation: The crossover in projectors responsible for KD negativity can correspond to a shift in population distribution among the eigenstates. That is, low-energy excitations start dominating different sectors depending on h_z/J, reflecting the reorganization of the system's dynamical response.

As the transverse field h_z is small, the time-evolved state predominantly occupies the lower-energy eigenstates of the post-quench Hamiltonian. This is consistent with the low value of the r-parameter ($r < 0.38$), indicating a nearly regular or integrable-like spectrum. In this regime, the negativity arises mainly from same-sector projectors, $|1\rangle\langle 1|$ and $|1\rangle\langle 1|$, and the first time KD negativity t_{neg} occurs relatively quickly, as interference develops efficiently within the lower-energy sector.

As h_z increases towards the crossover point ($h_z/J \sim 0.6$), the occupation probability begins to spread to higher-energy levels. At this stage, two energy levels are significantly occupied, corresponding to a shift in the projectors responsible for KD negativity to the cross-sector combination, $|1\rangle\langle 1|$ and $|0\rangle\langle 0|$. This change coincides with an increase in the r-parameter towards $r \approx 0.38$, reflecting the onset of spectral correlations that slow down the development of interference. Consequently, the first-negativity time t_{neg} exhibits a jump or sudden increase.

For larger $h_z > 0.6$, the occupation probability further spreads to include a third energy level, signaling that the system explores multiple sectors of the Hilbert space. The r-parameter continues to increase, showing

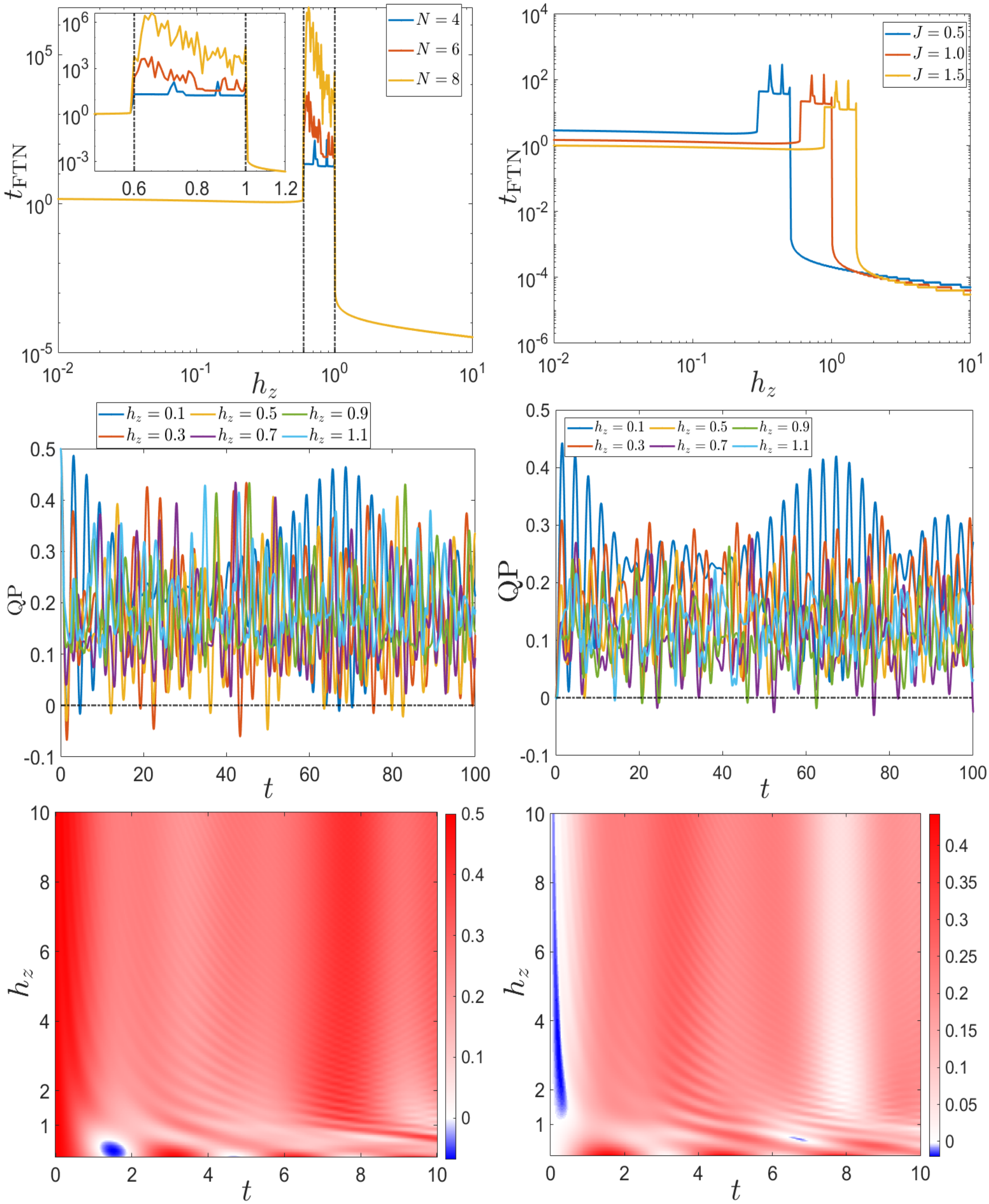

FIG. 1: Similar to Fig. ??(a) for the quenching case, we consider the all-down state in the z basis instead of the ground state. (a) t_l versus h_x with varying system size and (b) with varying interaction strength. value of t_l increases when $h_x/J = 3/5$ and other is sudden decrement when $h_x/J = 1$.

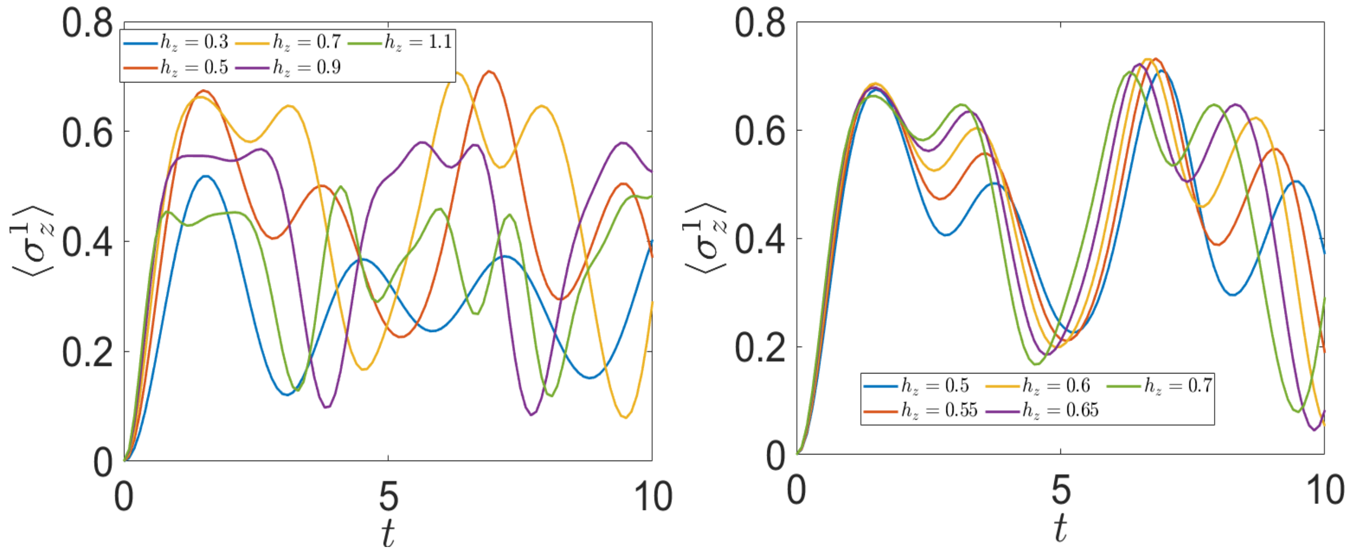

FIG. 2: Similar to Fig. ??(a) for the quenching case, we consider the all-down state in the z basis instead of the ground state. (a) t_l versus h_x with varying system size and (b) with varying interaction strength. value of t_l increases when $h_x/J = 3/5$ and other is sudden decrement when $h_x/J = 1$.

more spectral complexity, and the interference patterns responsible for KD negativity now involve multiple energy levels. This spreading of occupation across higher-energy states explains both the shift in projector sectors and the changes in t_{neg}. In summary, the evolution of occupation probabilities with h_z provides a microscopic picture of how spectral structure, captured by the r-parameter, governs the onset and nature of KD negativity in the system.

SPECTRAL r-PARAMETER

Consider a set of **sorted energy eigenvalues** of a quantum Hamiltonian:

$$\lambda_1 \le \lambda_2 \le \cdots \le \lambda_{2^N}.$$

Define the **level spacings**:

$$s_i = \lambda_{i+1} - \lambda_i > 0, \quad i = 1, 2, \ldots, 2^N - 1.$$

Then, the r-value for consecutive spacings is:

$$\tilde{r}_i = \frac{\min(s_i, s_{i-1})}{\max(s_i, s_{i-1})}, \quad i = 2, 3, \ldots, 2^N - 1.$$

The **average r-parameter** over all spacings is:

$$r = \frac{1}{2^N - 2} \sum_{i=2}^{2^N - 1} \tilde{r}_i.$$

Interpretation

- $r \approx 0.386 \Rightarrow$ Poisson statistics (integrable system)
- $r \approx 0.5307 \Rightarrow$ Gaussian Orthogonal Ensemble (GOE) statistics (chaotic system)

Use

The r-parameter measures spectral correlations and can quantify the **degree of chaos** in a quantum system.

The r-parameter is a widely used statistical indicator of quantum chaos. It characterizes the short-range correlations between consecutive energy level spacings of a Hamiltonian, without requiring any unfolding of the spectrum.

Given a set of ordered eigenvalues

$$\lambda_1 \le \lambda_2 \le \cdots \le \lambda_{2^N},$$

the nearest-neighbor spacings are defined as

$$s_i = \lambda_{i+1} - \lambda_i > 0, \qquad i = 1, 2, \ldots, 2^N - 1.$$

The ratio of consecutive spacings is

$$\tilde{r}_i = \frac{\min(s_i, s_{i-1})}{\max(s_i, s_{i-1})}, \qquad i = 2, 3, \ldots, 2^N - 1.$$

The averaged r-value is then

$$r = \frac{1}{2^N - 2} \sum_{i=2}^{2^N - 1} \tilde{r}_i.$$

Physical meaning

The quantity r serves as a spectral diagnostic revealing whether the system is chaotic or integrable:

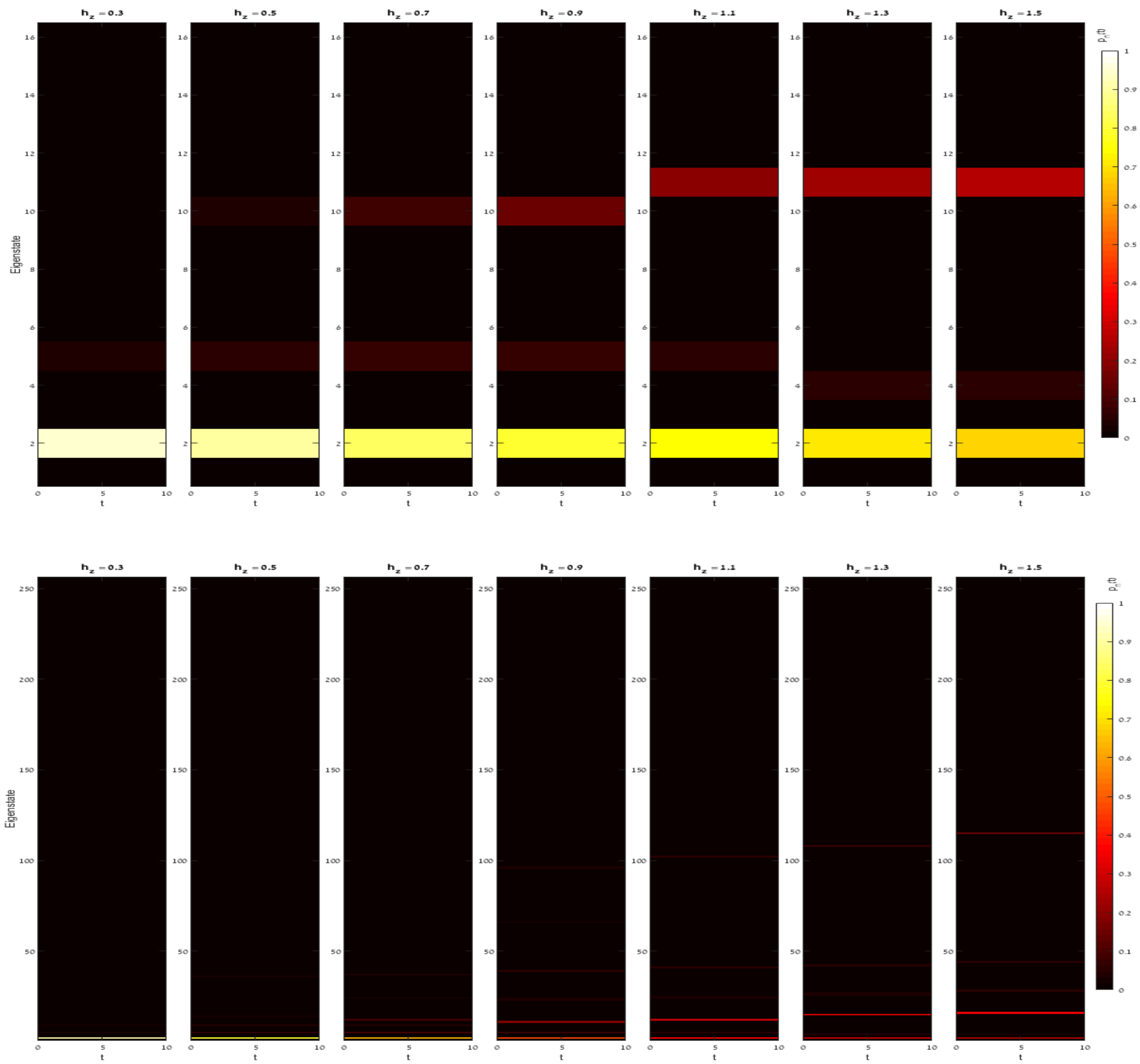

FIG. 3: Similar to Fig. ??(a) for the quenching case, we consider the all-down state in the z basis instead of the ground state. (a) t_l versus h_x with varying system size and (b) with varying interaction strength. value of t_l increases when $h_x/J = 3/5$ and other is sudden decrement when $h_x/J = 1$.

- **Chaotic (Wigner–Dyson statistics):** Energy levels repel each other, leading to stronger correlations in level spacings. The characteristic value is

$$r_{\mathrm{WD}} \approx 0.530.$$

- **Integrable (Poisson statistics):** Energy levels are uncorrelated and may cluster or cross, producing weak correlations and no level repulsion. The characteristic value is

$$r_{\mathrm{P}} \approx 0.386.$$

Thus, the r-parameter measures *how much level repulsion is present in the spectrum.* It identifies whether the post-quench Hamiltonian behaves like an integrable model or exhibits signatures of quantum chaos.

Use in the present work

In our system, the variation of r with the transverse field h_z/J indicates how the excitation spectrum reorganizes across the dynamical crossover. A sudden change in r correlates with changes in the projector responsible

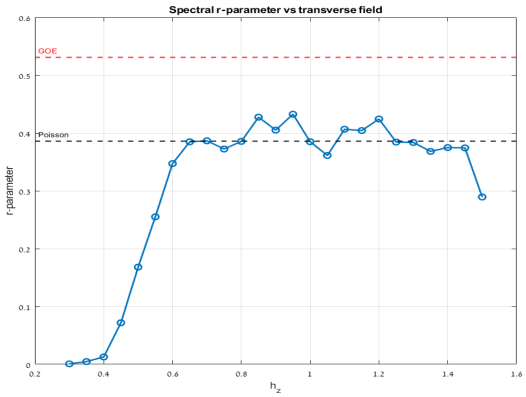

FIG. 4: Similar to Fig. **??**(a) for the quenching case, we consider the all-down state in the z basis instead of the ground state. (a) t_l versus h_x with varying system size and (b) with varying interaction strength. value of t_l increases when $h_x/J = 3/5$ and other is sudden decrement when $h_x/J = 1$.

for KD negativity, linking negativity generation to the underlying level statistics and spectral structure of the quench Hamiltonian.

The r-parameter is a spectral measure that characterizes the short-range correlations between consecutive energy levels of a quantum Hamiltonian. It is defined in terms of the ratio of consecutive level spacings,

$$\tilde{r}_i = \frac{\min(s_i, s_{i-1})}{\max(s_i, s_{i-1})},$$

where $s_i = \lambda_{i+1} - \lambda_i$ is the spacing between consecutive eigenvalues, and the average over all spacings gives

$$r = \frac{1}{2^N - 2} \sum_{i=2}^{2^N-1} \tilde{r}_i.$$

For integrable systems with uncorrelated energy levels, r tends to be low (approximately 0.38 or below), whereas for chaotic systems with level repulsion, r approaches the Wigner-Dyson value of around 0.53. In the context of our quench dynamics in the transverse-field Ising model, the r-parameter provides a useful diagnostic of how "regular" or "chaotic" the underlying spectrum is, and consequently, how the time evolution spreads the initial state across eigenstates.

We observe a direct connection between the value of r and the projectors responsible for generating Kirkwood-Dirac (KD) negativity. When $r < 0.38$, the system is in a regime where the spectrum is highly regular, corresponding to an almost integrable-like structure. In this case, the negativity arises predominantly from the same-sector projectors, $|1\rangle\langle 1|$ and $|1\rangle\langle 1|$. This indicates that the time-evolved state largely remains within a particular sector of the Hilbert space, and the interference required to produce negativity develops within this sector. However, as r approaches 0.38, the dominant negative contributions shift to cross-sector projectors, $|1\rangle\langle 1|$ and $|0\rangle\langle 0|$, reflecting that the time evolution now explores different sectors of the Hilbert space. The transition in the projectors corresponds to a reorganization of the low-energy excitations and the structure of quantum interference processes that give rise to negativity.

This spectral insight also connects naturally with the observed first time KD negativity, t_{neg}. In the integrable regime with $r < 0.38$, the negativity appears relatively quickly because the same-sector interference can develop efficiently. As r increases towards 0.38, the system requires more time to generate the appropriate interference patterns between different sectors, leading to a jump or increase in the first-negativity time. This behavior indicates that the spectral properties of the Hamiltonian, captured by the r-parameter, directly influence the timescale at which nonclassical quasiprobabilities first emerge. Therefore, by analyzing the r-parameter in conjunction with the projectors responsible for KD negativity, one can understand how the energy-level structure governs both the nature of interference processes and the dynamical onset of negativity in the system.

Connection between KD Negativity, Occupation Probabilities, and Spectral Structure

We investigate the first time at which the Kirkwood-Dirac (KD) quasiprobability becomes negative, t_{neg}, as a function of the transverse field h_z. For small h_z, the time-evolved state predominantly occupies the lower-energy eigenstates of the post-quench Hamiltonian. In this regime, the r-parameter, defined from consecutive energy level spacings as

$$\tilde{r}_i = \frac{\min(s_i, s_{i-1})}{\max(s_i, s_{i-1})}, \quad r = \frac{1}{2^N - 2} \sum_{i=2}^{2^N-1} \tilde{r}_i,$$

remains below 0.38, indicating a nearly regular, integrable-like spectral structure. Correspondingly, the negativity arises primarily from same-sector projectors, $|1\rangle\langle 1|$ and $|1\rangle\langle 1|$, and t_{neg} occurs relatively quickly, as interference develops efficiently within the lower-energy sector.

As h_z approaches the crossover value around $h_z/J \sim 0.6$, occupation probability begins to spread to higher-energy states. Two energy levels are now significantly populated, coinciding with a shift in the projectors responsible for KD negativity to the cross-sector combination, $|1\rangle\langle 1|$ and $|0\rangle\langle 0|$. The r-parameter increases towards $r \approx 0.38$, reflecting enhanced spectral correlations that reduce the efficiency of interference generation. Consequently, t_{neg} exhibits a sudden jump, corresponding to this dynamical crossover.

For larger $h_z > 0.6$, the occupation probability spreads further to include a third energy level, indicating that the system explores multiple sectors of the Hilbert space.

The r-parameter continues to grow, capturing the increased spectral complexity. In this regime, interference responsible for KD negativity involves multiple energy levels, explaining both the change in projector sectors and the variation of $t_{\rm neg}$. Thus, the evolution of occupation probabilities and the r-parameter provides a microscopic understanding of how the spectral structure governs the onset and nature of KD negativity across different quench strengths.

IMPACT AND IMPLICATIONS OF THE STUDY

Our analysis of the first-time Kirkwood-Dirac (KD) negativity, its dependence on the projector sectors, and the associated occupation probabilities provides several insights and practical benefits:

1. **Dynamical Quantum Phase Characterization:** The dependence of the first-time negativity $t_{\rm neg}$ on the transverse field h_z and the corresponding shift in the responsible projectors effectively defines a *dynamical crossover line* in the system. This provides a diagnostic tool to identify non-equilibrium phases or dynamical crossovers even in the absence of conventional order parameters. The approach is general and can be applied to other integrable or near-integrable quantum systems.

2. **Control of Nonclassicality:** The onset of KD negativity marks the emergence of nonclassical correlations. By understanding how $t_{\rm neg}$ depends on h_z and the underlying spectral structure, one can design quench protocols to achieve negativity at desired times. This has potential applications in *quantum sensing*, *weak measurement protocols*, and other quantum information processing tasks where early or strong nonclassical correlations are advantageous.

3. **Connection to Spectral Statistics and Quantum Chaos:** We find a direct relation between the r-parameter, which characterizes the level spacing statistics, and the projectors responsible for KD negativity. Systems with $r < 0.38$ tend to exhibit negativity via $|1\rangle\langle 1|$ projectors, while larger r values shift the negativity to $|1\rangle\langle 1|$ and $|0\rangle\langle 0|$ combinations. This provides a quantitative link between spectral properties and the dynamical emergence of nonclassicality, which can guide experimental studies in cold atoms, trapped ions, and superconducting qubits.

4. **Insight into Quench Dynamics:** The occupation probabilities indicate that for small h_z, the system largely populates lower-energy eigenstates. As h_z increases beyond $0.6J$, probability spreads to higher-energy levels, reflecting the reorganization of low-energy excitations. This microscopic insight into how the system explores the Hilbert space allows for the design of optimized quench protocols to control the onset and magnitude of KD negativity.

5. **Benchmarking Quantum Simulators:** The combination of first-time KD negativity, r-parameter analysis, and occupation dynamics provides a multi-faceted diagnostic toolkit. Experimentalists can measure one or more of these quantities to benchmark the performance of quantum simulators and validate their control over quench dynamics in spin chains and other many-body platforms.

In summary, our results demonstrate that first-time KD negativity, together with spectral and occupation information, offers a sensitive probe of the underlying dynamics, a tool for controlling nonclassical correlations, and a benchmark for quantum simulation platforms. These insights connect fundamental studies of quasiprobabilities to practical applications in quantum technology.

Connection between First-Time Negativity (FTN) and Energy Levels

a. Time evolution and energy gaps. The system evolves as

$$|\psi(t)\rangle = e^{-iHt}|\psi_0\rangle, \tag{12}$$

where H is the post-quench Hamiltonian. Expanding in the energy eigenbasis $\{|n\rangle\}$ of H:

$$|\psi(t)\rangle = \sum_n c_n e^{-iE_n t}|n\rangle, \quad c_n = \langle n|\psi_0\rangle. \tag{13}$$

The dynamics of quasiprobabilities depend on interference terms of the form

$$c_m^* c_n e^{i(E_m - E_n)t}, \tag{14}$$

i.e., differences in energy eigenvalues.

b. Role of energy gaps. If the initial state is mostly in low-energy eigenstates (small $E_n - E_m$), interference builds up slowly, delaying the first appearance of negativity. Conversely, if higher-energy states are significantly occupied or the spectrum has commensurate gaps, interference develops faster, leading to a smaller FTN.

c. Observations in the present system.

- For small h_z/J, the initial state overlaps mainly with the lowest-energy levels. Negativity arises later because interference terms take longer to become significant.

- For $h_z/J > 0.6$, higher-energy levels become occupied, causing interference between states with larger energy gaps. This results in negativity appearing at earlier times.

- Peaks or sharp changes in FTN often correspond to changes in the population of energy levels or level crossings/crossovers in the spectrum.

Connection between FTN and Energy Levels

Consider the time-evolved state after a quench:

$$|\psi(t)\rangle = e^{-iHt}|\psi_0\rangle, \tag{15}$$

where H is the post-quench Hamiltonian. Expanding in the energy eigenbasis $\{|n\rangle\}$ of H with eigenvalues E_n:

$$|\psi(t)\rangle = \sum_n c_n\, e^{-iE_n t}|n\rangle, \quad c_n = \langle n|\psi_0\rangle. \tag{16}$$

The Kirkwood-Dirac quasiprobability (or any Margenau-Hill type quasiprobability) can be written as

$$\begin{aligned} K_{ab}(t) &= \mathrm{Tr}\big[\Pi_a(t)\,\Pi_b\,\rho_0\big] \\ &= \sum_{m,n} c_m^* c_n\, e^{i(E_m-E_n)t}\,\langle m|\Pi_a|n\rangle\langle n|\Pi_b|\psi_0\rangle \end{aligned} \tag{17}$$

Negativity arises from the *interference terms* $c_m^* c_n e^{i(E_m-E_n)t}$ in the quasiprobability.

- If the initial state ψ_0 overlaps mostly with **low-energy levels** (i.e., c_n significant only for small E_n), the phase differences $E_m - E_n$ are small. Consequently, interference builds up slowly, and the first-time negativity (FTN) occurs later.
- If **higher-energy levels** are also occupied (c_n significant for larger E_n), the phase differences are larger. Interference develops faster, leading to an earlier FTN.

E. Derivation of Kirkwood-Dirac quasiprobability in the energy eigenbasis

The Kirkwood-Dirac (KD) quasiprobability for a system with initial state $\rho_0 = |\psi_0\rangle\langle\psi_0|$ and two projectors $\Pi_a(t)$ and Π_b is defined as:

$$K_{ab}(t) = \mathrm{Tr}\big[\Pi_a(t)\,\Pi_b\,\rho_0\big], \tag{18}$$

where $\Pi_a(t)$ is in the Heisenberg picture, $\Pi_a(t) = e^{iHt}\Pi_a e^{-iHt}$, and Π_b is time-independent.

Let $\{|n\rangle\}$ be the eigenstates of the post-quench Hamiltonian H with eigenvalues E_n:

$$H|n\rangle = E_n|n\rangle. \tag{19}$$

Then the Heisenberg evolution of Π_a in this basis is

$$\langle m|\Pi_a(t)|n\rangle = e^{i(E_m-E_n)t}\langle m|\Pi_a|n\rangle. \tag{20}$$

By definition, the trace of any operator O is the sum of its diagonal elements in a complete orthonormal basis $\{|m\rangle\}$:

$$\mathrm{Tr}[O] = \sum_m \langle m|O|m\rangle. \tag{21}$$

This is true for any operator and any complete orthonormal basis. Using a complete set of eigenstates $\sum_n |n\rangle\langle n| = \mathbf{1}$, we can write the trace as

$$K_{ab}(t) = \sum_m \langle m|\Pi_a(t)\Pi_b\rho_0|m\rangle = \sum_{m,n}\langle m|\Pi_a(t)|n\rangle\langle n|\Pi_b\rho_0|m\rangle. \tag{22}$$

Inserting $\rho_0 = |\psi_0\rangle\langle\psi_0|$ and defining $c_m = \langle m|\psi_0\rangle$, we get

$$\langle n|\Pi_b\rho_0|m\rangle = \langle n|\Pi_b|\psi_0\rangle\langle\psi_0|m\rangle = \langle n|\Pi_b|\psi_0\rangle\, c_m^*. \tag{23}$$

Combining these expressions, the KD quasiprobability becomes

$$K_{ab}(t) = \sum_{m,n} c_m^* c_n\, e^{i(E_m-E_n)t}\,\langle m|\Pi_a|n\rangle\langle n|\Pi_b|\psi_0\rangle. \tag{24}$$

Physical interpretation:

- $c_m^* c_n$ are amplitudes from the initial state.
- $e^{i(E_m-E_n)t}$ represents the interference between energy levels.
- $\langle m|\Pi_a|n\rangle\langle n|\Pi_b|\psi_0\rangle$ are the matrix elements of the projectors.
- Negativity in the KD quasiprobability arises due to the interference terms, and the first-time negativity (FTN) depends on the distribution of initial occupation among low- and high-energy eigenstates.

BELL-PAIR TENSOR-PRODUCT STATE

We consider an N-qubit entangled state constructed from repeated copies of the Bell state

$$|\Phi^+\rangle = \frac{1}{\sqrt{2}}\left(|00\rangle + |11\rangle\right). \tag{25}$$

If the total number of qubits is N and we pair them into $N/2$ Bell pairs, then the global state is given by

$$|\Psi_N\rangle = |\Phi^+\rangle \otimes |\Phi^+\rangle \otimes \cdots \otimes |\Phi^+\rangle, \tag{26}$$

where the tensor product contains $\frac{N}{2}$ identical Bell states.

Explicitly,

$$|\Psi_N\rangle = \frac{1}{2^{N/4}}\left(|00\rangle + |11\rangle\right)^{\otimes\frac{N}{2}}. \tag{27}$$

Description

The state $|\Psi_N\rangle$ represents a system of N qubits organized into $\frac{N}{2}$ independent maximally entangled pairs. Each pair $(2k-1, 2k)$ is in the Bell state $|\Phi^+\rangle$, meaning:

- The qubits inside each pair are **maximally entangled**.

- Different pairs are **not entangled with each other**, but each Bell pair contains quantum correlations that cannot be written as a product of individual qubit states.
- The total entanglement in the system grows linearly with the number of Bell pairs.

This structure is useful when studying:

- multipartite entanglement building blocks,
- entanglement propagation in many-body dynamics,
- entanglement-assisted protocols,
- benchmarking of quantum circuits.

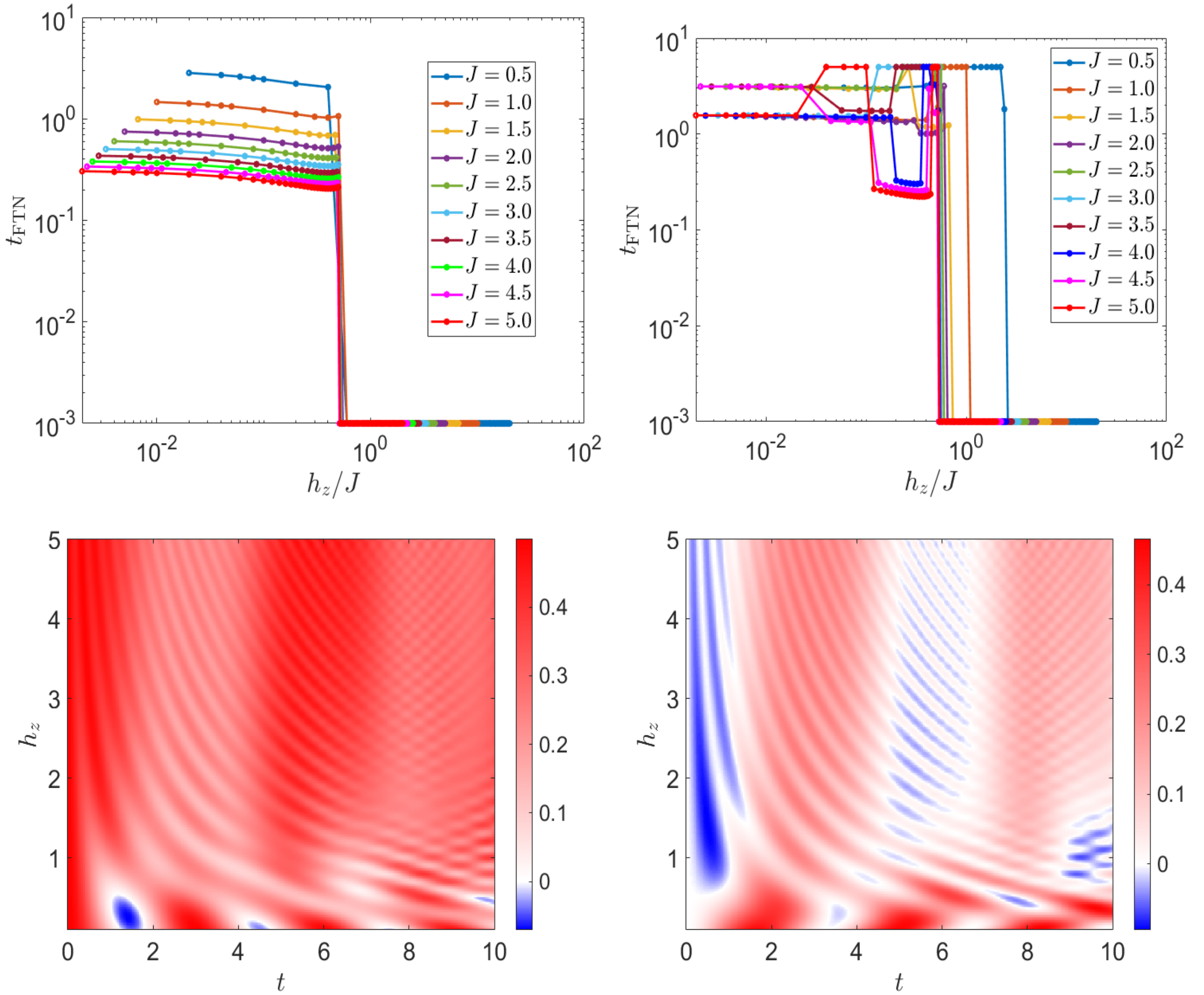

FIG. 5: Similar to Fig. **??**(a) for the quenching case, we consider the all-down state in the z basis instead of the ground state. (a) t_l versus h_x with varying system size and (b) with varying interaction strength. value of t_l increases when $h_x/J = 3/5$ and other is sudden decrement when $h_x/J = 1$.